metal carbonyl moiety in the end on fashion is probably a result of steric factors.

**Acknowledgment.** We thank the National Science Foundation for financial support.

**Supplementary Material Available:** Tables of crystal data, atom coordinates, thermal parameters, bond distances and angles, and hydrogen coordinates (11 pages); listings of structure factors (34 pages). Ordering information is given on any current masthead page.

# Preparation and Physical Properties of Trinuclear Oxo-Centered Manganese Complexes of the General Formulation $[Mn_3O(O_2CR)_6L_3]^{0,+}$ (R = Me or Ph; L = a Neutral Donor Group) and the Crystal Structures of $[Mn_3O(O_2CMe)_6(pyr)_3](pyr)$ and $[Mn_3O(O_2CPh)_6(pyr)_2(H_2O)]\cdot 0.5MeCN$

**John B. Vincent,[†] Hsiu-Rong Chang,[§] Kirsten Folting,[‡] John C. Huffman,[‡] George Christou,*[†] and David N. Hendrickson*[§]**

*Contribution from the Department of Chemistry and the Molecular Structure Center, Indiana University, Bloomington, Indiana 47405, and the School of Chemical Sciences, University of Illinois, Urbana, Illinois 61801.* *Received October 15, 1986*

**Abstract:** The reaction of N-*n*-$Bu_4MnO_4$ with appropriate reagents in nonaqueous solvents leads to the high-yield formation of trinuclear oxo-centered Mn complexes of general formulation $[Mn_3O(O_2CR)_6L_3]^{z+}$ (**1**, R = Me, L = pyr, $z$ = 1; **2**, R = Me, L = pyr, $z$ = 0, monopyridine solvate; **3**, R = Me, L = pyr, $z$ = 0, unsolvated; **4**, R = Ph, $L_3$ = $(pyr)_2(H_2O)$, $z$ = 0; **5**, R = Me, L = HIm, $z$ = 1; pyr = pyridine, HIm = imidazole). The crystal structures of complexes **2** and **4** have been determined. Complex **2** crystallizes in rhombohedral space group R32 with (at −50 °C) $a = b$ = 17.552 (6) Å, $c$ = 10.918 (3) Å, $\gamma$ = 120.00 (1)°, and $Z$ = 3. A total of 1546 unique data with $F > 3\sigma(F)$ were refined to conventional values of $R$ and $R_w$ of 5.77 and 5.86%, respectively. Complex **4** crystallizes in monoclinic space group $P2_1$ with (at −156 °C) $a$ = 15.058 (10) Å, $b$ = 23.600 (17) Å, $c$ = 14.959 (10) Å, $\beta$ = 91.01 (3)°, and $Z$ = 2. A total of 7174 unique data with $F > 3\sigma$ ($F$) were refined to values of $R$ and $R_w$ of 8.64 and 8.43%, respectively. Both **2** and **4** possess an oxo-centered $Mn_3O$ unit characteristic of "basic carboxylates" with peripheral ligation provided by bridging carboxylate and terminal pyr (or $H_2O$) groups. Each Mn is distorted octahedral, and consideration of overall charge of the trinuclear units necessitates a mixed-valence $Mn^{II}Mn_2^{III}$ description. In **2**, the presence of a $C_3$ axis through the central O and perpendicular to the $Mn_3O$ unit necessitates the Mn centers to be crystallographically equivalent, suggesting rapid *intra*molecular electron transfer or electronic delocalization. In contrast, **4** possesses no imposed symmetry elements and is in a trapped-valence situation in accord with its mixed-ligand nature, since two Mn centers have a terminal pyr group while the third Mn has a terminal $H_2O$ molecule. The latter metal center is assigned as the $Mn^{II}$ ion based on its longer metal–ligand distances. Variable temperature solid state magnetic susceptibility studies have been performed on **1**–**4** in the temperature range of ~6 to ~340 K. Satisfactory fits to the observed susceptibility data have been obtained by assuming isotropic magnetic exchange interactions and employing the appropriate spin Hamiltonians and derived susceptibility equations. All Mn centers are shown to be in high-spin electronic configurations and to be antiferromagnetically coupled. The derived exchange parameters are all relatively small in magnitude, $|J| < 11$ cm$^{-1}$. In addition, it is found that the antiferromagnetic exchange interactions are smaller for the $Mn_3O$ units than those for isostructural $Fe_3O$ systems, and a rationalization is proposed. Since phase transitions had previously been characterized by heat capacity measurements on $[Fe_3O(O_2CMe)_6(pyr)_3](pyr)$, isostructural complex **2** was investigated by differential scanning calorimetry (DSC) in the temperature range 153–303 K. An exothermic thermal effect is clearly evident with a peak at 184.7 K in the cooling curve (the other mixed-valence $Mn_3O$ systems showed no thermal effects in their DSC thermograms). The origin of this thermal effect and comparisons with the corresponding behavior of the Fe complex are described.

Interest in trinuclear $\mu_3$-oxo-bridged manganese complexes of general composition $[Mn_3O(O_2CR)_6L_3]$ draws from three quarters. First, there is a need to characterize polynuclear manganese complexes as models for the water oxidation center of photosynthetic electron transport chains. A cluster of two to four manganese ions is known to catalyze the oxidation of two $H_2O$ molecules to give one $O_2$ molecule.[1] Second, a comparison of the *intra*molecular electron transfer characteristics of mixed-valence $Mn_3O$ complexes with those of the reasonably well-characterized $Fe_3O$ analogues would be instructional. The electronic coupling between Mn ions in the $Mn_3O$ complexes should be weaker than that found for the mixed-valence $Fe_3O$ complexes. Third, the magnetic exchange interaction characteristics of the mixed-valence $Mn_3O$ complexes need to be compared to those of the $Fe_3O$ analogues.

Trinuclear $\mu_3$-oxo-bridged iron acetate complexes have been studied in great detail,[2-7] whereas analogous mixed-valence

[†] Indiana University, Department of Chemistry.
[‡] Indiana University, Molecular Structure Center.
[§] University of Illinois.

(1) (a) Amesz, J. *Biochim. Biophys. Acta* **1983**, *726*, 1. (b) Govindjee; Kambara, T.; Coleman, W. *Photochem. Photobiol.* **1985**, *42*, 187. (c) Dismukes, G. C. *Photochem. Photobiol.* **1986**, *43*, 99.
(2) (a) Oh, S. M.; Hendrickson, D. N.; Hassett, K. L.; Davis, R. E. *J. Am. Chem. Soc.* **1984**, *106*, 7984. (b) Oh, S. M.; Hendrickson, D. N.; Hassett, K. L.; Davis, R. E. *J. Am. Chem. Soc.* **1985**, *107*, 8009.

0002-7863/87/1509-5703$01.50/0 

manganese–acetate complexes have been the object of only limited investigation to date. In a preliminary communication[8] of the room temperature structure, $[Mn_3O(O_2CMe)_6(pyr)_3](pyr)$ (pyr is pyridine) has been shown to crystallize in space group R32. The presence of a $C_3$ axis led the authors to conclude that all three manganese ions are equivalent; the position of the pyridine solvate molecule was not reported. In another communication,[9] $[Mn_3O(O_2CMe)_6(3\text{-Cl-pyr})_3]$ was described as valence trapped (space group $P2_1/a$) with one $Mn^{II}$ and two $Mn^{III}$ ions. The atomic coordinates for this compound obtained from the Cambridge Crystallographic Data Centre show that there is a disordered 3-Cl-pyr solvate molecule present as well. The importance of the solvate molecules will be discussed below.

To increase our sparse knowledge in this area, we have sought the preparation of $Mn_3O$ complexes. Recently, we described how N-*n*-$Bu_4MnO_4$ was proving to be a useful reagent for the synthesis of Mn complexes in nonaqueous solvents and described its use to prepare a complex containing the bisphenoxo-bridged $Mn_2^{III}$ dimer unit $[Mn_2(sal)_4(pyr)_2]^{2-}$ (sal is salicylate).[10] We can now report that various complexes containing the desired $Mn_3O$ core are also obtainable from this reagent. In this paper are described the results of this synthetic work, together with single-crystal X-ray structures of two mixed-valence $Mn_3O$ complexes and the results of variable-temperature magnetic susceptibility and differential scanning calorimetry (DSC) measurements.

## Experimental Section

**Compound Preparation.** All chemicals and solvents were used as received; all preparations were performed under aerobic conditions.

**N-*n*-$Bu_4MnO_4$.** This material was prepared, as outlined in the literature,[11] by mixing aqueous solutions of $KMnO_4$ (5.00 g, 31.6 mmol) and N-*n*-$Bu_4Br$ (12.00 g, 37.2 mmol) with vigorous stirring to give a total volume of ca. 200 mL. The immediate purple precipitate was collected by filtration, washed thoroughly with distilled water and diethyl ether, and dried in vacuo *at ambient temperature*: yield >90%.

**Warning.** There have been reports of the detonation of quaternary ammonium permanganates during drying at elevated temperatures.[12-15] A systematic study[15] has shown that salts containing unsaturated groups will explode at 80 °C or above. N-*n*-$Bu_4^+$ or $NEt_4^+$ salts will also decompose at these temperatures but not explosively. We recommend appropriate care be taken in the use of organic permanganates. Further, the N-*n*-$Bu_4^+$ or $NEt_4^+$ salts should be used where possible and dried in vacuo at room temperature, as described above. We have found N-*n*-$Bu_4MnO_4$ to be pure enough for use without recrystallization, and storage in a refrigerator increases its stability to a slow decomposition over several weeks at room temperature to yield a brown sticky solid.

**$[Mn_3O(O_2CMe)_6(pyr)_3](ClO_4)$ (1).** $Mn(O_2CMe)_2{\cdot}4H_2O$ (2.00 g, 8.15 mmol) was dissolved in a solvent mixture comprising absolute EtOH (20 mL), pyridine (3 mL), and glacial acetic acid (12 mL). The resulting solution was stirred while solid N-*n*-$Bu_4MnO_4$ (1.14 g, 3.15 mmol) was added in small portions to give a deep brown homogeneous solution. Addition of $NaClO_4$ (0.69 g, 5.65 mmol) yielded, after a few minutes, a brown microcrystalline precipitate which was collected by filtration, washed copiously with EtOH, and dried in vacuo; yield 60% based on total available Mn. Recrystallization from acetone yields gold needles: IR data 3100 (w), 1610 (vs), 1340 (m), 1220 (s), 1160 (w), 1090 (vs), 1070 (s), 1045 (s), 1015 (s), 940 (w), 770 (s), 690 (s), 660 (s), 645 (m), 610 (s), 585 (w), 515 (w), 440 (m), 380 (m, br), 285 (m); $\lambda_{max}$ ($\epsilon_M$) in MeOH 289 (2640), 448 (264), 478 (sh, 238), 560 (sh, 91). Anal. Calcd for $C_{27}H_{33}N_3O_{17}ClMn_3$: C, 37.20; H, 3.82; N, 4.82. Found: C, 37.12; H, 3.99; N, 4.56.

**$[Mn_3O(O_2CMe)_6(pyr)_3]{\cdot}pyr$ (2).** $Mn(O_2CMe)_2{\cdot}4H_2O$ (2.00 g, 8.15 mmol) was dissolved in a solvent mixture comprising glacial acetic acid (10 mL) and pyridine (20 mL). The resulting solution was stirred while solid N-*n*-$Bu_4MnO_4$ (0.76 g, 2.10 mmol) was added in small portions to yield a deep brown/black homogeneous solution. This was allowed to stand undisturbed for 48 h, and the resulting large octahedral-shaped crystals were collected by filtration, washed with pyridine, and dried in vacuo; yield ~65% based on total manganese. Recrystallization can be effected by slowly cooling a warm pyridine solution: IR data 1615 (vs), 1330 (m), 1220 (s), 1150 (m), 1070 (s), 1040 (s, d), 1010 (s, d), 930 (w), 750 (s), 710 (m), 690 (vs), 650 (vs), 615 (w), 610 (m), 540 (m, br), 440 (m), 410 (w), 350 (m), 300 (w), 270 (m); $\lambda_{max}$ ($\epsilon_M$) in MeCN 263 (5520), 438 (320). Anal. Calcd for $C_{32}H_{38}N_4O_{13}Mn_3$: C, 45.14; H, 4.50; N, 6.58. Found: C, 44.87; H, 4.30; N, 6.27.

**$Mn_3O(O_2CMe)_6(pyr)_3$ (3).** Complex **1** was dissolved in MeCN, and the solution was allowed to slowly concentrate by evaporation. This yielded black crystals which were collected by filtration, washed with ether, and dried in vacuo: yield ca. 60%. Anal. Calcd for $C_{27}H_{33}N_3O_{13}Mn_3$: C, 41.99; H, 4.31; N, 5.44. Found: C, 42.27; H, 4.57; N, 5.68.

**$[Mn_3O(O_2CPh)_6(pyr)_2(H_2O)]{\cdot}0.5MeCN$ (4).** $Mn(O_2CMe)_2{\cdot}4H_2O$ (2.00 g, 8.15 mmol) and benzoic acid (7.50 g, 61.4 mmol) were dissolved in pyridine (3 mL) and absolute EtOH (20 mL), and solid N-*n*-$Bu_4MnO_4$ (1.14 g, 3.15 mmol) was added in small portions with stirring to give a brown homogeneous solution. After 24 h, the resulting grey-green precipitate was filtered, washed with EtOH, and dried in vacuo. The crude yield was >95%. Recrystallization was accomplished by allowing an MeCN solution to slowly concentrate by evaporation to give deep green crystals, which were collected by filtration, washed with EtOH, and dried in vacuo: yield 60%; IR data 3450 (w, br), 3080 (w, br), 2220 (w), 1620 (vs), 1570 (vs), 1485 (m), 1220 (s), 1175 (s), 1150 (m), 1120 (w), 1070 (s), 1040 (s), 1030 (m), 1020 (s), 1010 (w), 970 (w), 930 (w), 835 (m), 810 (w), 765 (m), 720 (vs), 690 (s), 670 (s), 640 (m), 620 (w), 595 (w), 545 (w, br), 450 (m, br), 320 (m), 260 (m); $\lambda_{max}$ ($\epsilon_M$) in MeCN 280 (sh, 7720), 484 (376). Anal. Calcd for $C_{53}H_{41.5}N_{2.5}O_{14}Mn_3$: C, 57.65; H, 3.97; N, 3.17; Mn, 14.93. Found: C, 57.80; H, 4.14; N, 2.93; Mn, 14.06.

**$[Mn_3O(O_2CMe)_6(HIm)_3](O_2CMe){\cdot}DMF$ (5).** Imidazole (2.50 g, 36.7 mmol) and $Mn(O_2CMe)_2{\cdot}4H_2O$ (2.00 g, 8.15 mmol) were dissolved in a solvent mixture comprising glacial acetic acid (12 mL) and di-

**Table I.** Crystallographic Data for **2** and **4**

| | **2** | **4** |
|---|---|---|
| formula | $C_{27}H_{33}N_3O_{13}Mn_3$ | $2\times C_{52}H_{42}N_2O_{14}Mn_3$ |
| molar mass | 772.38 | 1083.74 |
| cryst system | rhombohedral | monoclinic |
| space group | R32 | $P2_1$ |
| temp, °C | −50 | −156 |
| *a*, Å | 17.552 (6)[a] | 15.058 (10)[b] |
| *b*, Å | 17.552 (6) | 23.600 (17) |
| *c*, Å | 10.918 (3) | 14.959 (10) |
| $\beta$, deg | | 91.01 (3) |
| $\gamma$, deg | 120.00 (1) | |
| *Z* | 3 | 2 |
| vol., Å$^3$ | 2913.58 | 5315.10 |
| cryst size, mm | 0.30 × 0.30 × 0.19 | 0.30 × 0.20 × 0.30 |
| radiatn (Mo K$\alpha$), Å | 0.71069[c] | 0.71069[c] |
| abs coeff. cm$^{-1}$ | 9.764 | 7.395 |
| scan speed, deg min$^{-1}$ | 4 ($\theta/2\theta$) | 4 ($\theta/2\theta$) |
| scan width, deg | 2.0 + dispersion | 1.6 + dispersion |
| total data | 1871 | 8592 |
| unique data | 1546 | 7174 |
| averaging *R* | 0.025[d] | 0.078[e] |
| obsd data, $F > 3\sigma(F)$ | 616 | 4216 |
| *R* ($R_w$), % | 5.77 (5.86)[f] | 8.64 (8.43)[f] |
| goodness of fit | 1.449 | 1.360 |

[a] Reflections (24) at −50 °C. [b] Reflections (38) at −156 °C. [c] Graphite monochromator. [d] Reflections (197) measured more than once. [e] Reflections (1279) measured more than once. [f] No absorption correction performed.

(3) Sorai, M.; Kaji, K.; Hendrickson, D. N.; Oh, S. M. *J. Am. Chem. Soc.* **1986**, *108*, 702.
(4) Woehler, S. E.; Wittebort, R. J.; Oh, S. M.; Hendrickson, D. N.; Inniss, D.; Strouse, C. E. *J. Am. Chem. Soc.* **1986**, *108*, 2938.
(5) Hendrickson, D. N.; Oh, S. M.; Doug, T.-Y.; Kambara, T.; Cohn, M. J.; Moore, M. F. *Comm. Inorg. Chem.* **1985**, *4*, 329.
(6) (a) Woehler, S. E.; Wittebort, R. J.; Oh, S. M.; Kambara, T.; Hendrickson, D. N.; Inniss, D.; Strouse, C. E. *J. Am. Chem. Soc.* **1987**, *109*, 1063. (b) Oh, S. M.; Wilson, S. R.; Hendrickson, D. N.; Woehler, S. E.; Wittebort, R. J.; Inniss, D.; Strouse, C. E. *J. Am. Chem. Soc.* **1987**, *109*, 1073.
(7) Kambara, T.; Hendrickson, D. N.; Sorai, M.; Oh, S. M. *J. Chem. Phys.* **1986**, *85*, 2895.
(8) Baikie, A. R. E.; Hursthouse, M. B.; New, D. B.; Thornton, P. *J. Chem. Soc., Chem. Commun.* **1978**, 62.
(9) Baikie, A. R. E.; Hursthouse, M. B.; New, L.; Thornton, P.; White, R. G. *J. Chem. Soc., Chem. Commun.* **1980**, 684.
(10) Vincent, J. B.; Folting, K.; Huffman, J. C.; Christou, G. *Inorg. Chem.* **1986**, *25*, 996.
(11) Sala, T.; Sargent, M. V. *J. Chem. Soc., Chem. Commun.* **1978**, 253.
(12) Morris, J. A.; Mills, D. C. *Chem. Br.* **1978**, *14*, 326.
(13) Jager, M.; Lutolf, J.; Meyer, M. W. *Angew. Chem., Int. Ed. Engl.* **1979**, *18*, 786.
(14) Schmidt, H.-J.; Schafer, H. J. *Angew. Chem., Int. Ed. Engl.* **1979**, *18*, 787.
(15) Leddy, B. P.; McKervey, M. A.; McSweeney, P. *Tetrahedron Lett.* **1980**, *21*, 2261.

methylformamide (DMF) (25 mL). To this was slowly added a solution of N-*n*-$Bu_4MnO_4$ (1.14 g, 3.15 mmol) in DMF (5 mL) to yield a red-brown solution. Precipitation of gold microcrystals of the DMF monosolvate began within a few minutes and was complete after about 15 min. The solid was collected by filtration, washed with ether, and dried in vacuo; yield 70%. Anal. Calcd for $C_{26}H_{40}N_7O_{16}Mn_3$: C, 35.83; H, 4.63; N, 11.25. Found: C, 35.80; H, 4.48; N, 11.17. Recrystallization from MeOH/ether gave red-orange crystals of the unsolvated complex. IR data 3150 (s), 3030 (w, br), 1615 (vs), 1260 (m), 1190 (m), 1140 (s), 1100 (m), 1070 (s), 1045 (w), 1025 (s), 960 (s), 940 (m), 885 (m), 840 (s), 750 (s), 670 (s), 655 (vs), 610 (s), 600 (s), 595 (sh), 550 (w), 515 (w), 480 (w), 390 (s), 375 (m), 310 (s), 280 (m), 225 (m); $\lambda_{max}$ ($\epsilon_M$) in MeOH 291 (2540), 464 (295). Anal. Calcd for $C_{23}H_{33}N_6O_{15}Mn_3$: C, 34.60; H, 4.17; N, 10.53. Found: C, 34.52; H, 4.31; N, 10.89.

**X-ray Crystallography.** Data were collected at −50 and −156 °C for **2** and **4**, respectively. Details of the diffractometry, low-temperature facilities, and computational procedures employed by the Molecular Structure Center have been described elsewhere.[16] Pertinent parameters are listed in Table I. Structures were solved by a combination of direct methods (MULTAN) and Fourier techniques.

For complex **2**, data were collected at −50 °C to avoid problems associated with a phase transition at lower temperatures. The structure was refined in space group R32 as in the previous structural determination of this material.[8] When the non-hydrogen atoms of the $Mn_3O(O_2CMe)_6(pyr)_3$ unit had been located, a difference Fourier indicated the pyridine solvate molecule lying on, and seriously disordered about, the $C_3$ axis. The plane of the pyridine ring is essentially parallel to the $C_3$ axis and perpendicular to the $Mn_3$ plane. All non-hydrogen atoms, with the exception of the disordered pyridine, were refined with anisotropic thermal parameters. Refinement was by full-matrix least squares. In the final refinement cycles, the positions of all hydrogen atoms, except those in the disordered solvate, were calculated and placed in fixed idealized positions (C–H = 0.95 Å). The hydrogen atoms were assigned thermal parameters of 1 + $B_{iso}$ of the carbon atom to which they were bound. A final difference Fourier was quite featureless, with the largest peak being 0.30 e/Å$^3$.

For complex **4**, a systematic search of a limited hemisphere of reciprocal space yielded a set of reflections which exhibited monoclinic symmetry. The only observed systematic extinction was that of $0k0$ for $k = 2n + 1$, leaving the choice of two possible space groups $P2_1$ or $P2_1/m$. The choice of the noncentrosymmetric space group $P2_1$ was confirmed by the successful solution and refinement of the structure. The asymmetric unit contains two complete $Mn_3$ units as well as three molecules of MeCN solvates. Due to the large number of atoms (151), no attempts were made to locate or include hydrogen atoms in the refinement. For the same reason, only the Mn atoms were refined by using anisotropic thermal parameters; all other atoms were refined in a cyclical fashion by using isotropic thermal parameters. Since the space group is noncentrosymmetric, an attempt was made at determining the correct handedness by refining the inverse structure. The resulting $R$ value (0.087) was slightly larger, and we, therefore, conclude that we have the correct handedness or that a distinction is impossible. The final difference Fourier was essentially featureless, with the largest peak being 0.73 e/Å$^3$.

**Physical Measurements.** Variable temperature magnetic susceptibility data were measured by using a series 800 VTS-50 SQUID susceptometer (S.H.E. Corp.), maintained by the Physics Department at the University of Illinois. The susceptometer was operated at a magnetic field strength of 10 kG. Diamagnetic corrections were estimated from Pascal's constants and subtracted from the experimental susceptibility data to obtain the molar paramagnetic susceptibilities of the compounds. These molar paramagnetic susceptibilities were fit to the appropriate theoretical expressions by means of a least-squares-fitting computer program.[17]

Differential scanning calorimetry (DSC) data were measured for a crystalline sample of $[Mn_3O(O_2CMe)_6(pyr)_3](pyr)$ by means of a Perkin-Elmer DSC-7 differential scanning calorimeter equipped with a Perkin-Elmer TAC-7 instrument controller which is interfaced to a Perkin-Elmer 7500 professional computer and Perkin-Elmer graphics plotter Model 2. Measurements were carried out on a ~15-mg sample employing heating and cooling rates from 5 to 10 deg/min.

Infrared and electronic spectra were recorded on Perkin-Elmer Model 283 and Hewlett-Packard Model 4450A spectrophotometers, respectively.

## Results and Discussion

**Synthesis and Structures.** Prior reports of the synthesis and properties of trinuclear oxo-centered Mn complexes are few.[8,9,18-20]

**Table II.** Fractional Coordinates and Isotropic Thermal Parameters for **2**[a]

| atom | $x$ | $y$ | $z$ | $B_{iso}$ |
|---|---|---|---|---|
| Mn(1) | 8897 (1) | 8897[b] | 0[b] | 38 |
| O(2) | 0[b] | 0[b] | 0[b] | 36 |
| O(3) | 4007 (4) | 5611 (4) | 5373 (6) | 54 |
| C(4) | 5074 (6) | 3284 (6) | 5029 (9) | 51 |
| O(5) | 5768 (5) | 4105 (4) | 1926 (6) | 57 |
| C(6) | 52 (10) | 7880 (11) | 2697 (16) | 115 |
| N(7) | 7662 (5) | 7662[b] | 0[b] | 45 |
| C(8) | 3561 (6) | 997 (6) | 3216 (9) | 55 |
| C(9) | 5881 (7) | 6445 (7) | 3489 (12) | 62 |
| C(10) | 6132 (10) | 6132[b] | 0[b] | 124 |
| C(11) | 0[b] | 0[b] | 3781 (57) | 87 (25) |
| C(12) | 587 (35) | 10158 (36) | 4142 (48) | 109 (19) |
| C(13) | 3025 (90) | 7049 (59) | 2123 (86) | 157 (44) |

[a] Coordinates are ×10$^4$; $B_{iso}$ values are ×10. [b] Parameters were not varied.

Synthetic procedures have almost invariably employed polymeric "$Mn^{III}$ acetate", $[Mn_3O(O_2CMe)_6\cdot(O_2CMe)(HO_2CMe)]_n$, which can be readily obtained from the oxidation of $Mn(O_2CMe)_2\cdot 4H_2O$ with $KMnO_4$ in hot glacial acetic acid.[19] Reaction of this material with excess of a neutral donor group L led to discrete units of formulation $[Mn_3O(O_2CMe)_6L_3]^z$ ($z = +1$, L = pyr, 2-picoline; $z = 0$, L = pyr, *p*-Cl-pyr); the structures of the $z = 0$ pair have been communicated.[8,9]

As part of our continuing development of N-*n*-$Bu_4MnO_4$ as a reagent for inorganic syntheses in nonaqueous solvents, we have explored its use for synthesis of $Mn_3O$-type complexes and have found that it works extremely well. Thus, high yields of tractable crystalline materials have been isolated under straightforward one-pot reaction conditions and ambient temperatures. Solvents of choice are EtOH, DMF, and pyridine which ensure solubility of all reactants; cleanest reactions are obtained when an excess of carboxylic acid is also present, otherwise low yields or intractable brown gel-like precipitates result. Our synthetic strategy has been to react together particular ratios of $Mn^{VII}$:$Mn^{II}$ to yield products in the intermediate +2.67 to +3.00 metal oxidation state range characteristic of $Mn_3O$ units. After some preliminary experimentation, the procedures described in the Experimental Section have been found to give consistently pure and high yield products; we have by no means explored all possible combinations of solvents and reagent ratios and, consequently, do not claim these procedures to have been optimized. However, we have noticed that small changes to the $Mn^{VII}$:$Mn^{II}$ ratios have no noticeable effect on the identity of the products or their yields; as we noted previously,[10] redox reactions involving solvent, atmospheric oxygen, or reagent impurities could compensate for excess or lack of $Mn^{II}$, for example, over that required to yield the preferred product. A $Mn^{VII}$:$Mn^{II}$ ratio of 3.15:8.15 has now become our routinely used stoichiometry and has provided access to complexes **1**, **4**, and **5**. This ratio should, in theory, provide an average metal oxidation of +3.39 according to eq 1 but cleanly leads instead to either

$$3.15Mn^{7+} + 8.15Mn^{2+} \rightarrow 11.30Mn^{3.39+} \quad (1)$$

$Mn_2^{III}Mn^{II}$ species **4**, or $Mn_3^{III}$ species **1** and **5**. Since it is known from the literature that the reduced form of **1** exists,[8] i.e., complex **2**, we sought its synthesis by lowering the $Mn^{VII}$:$Mn^{II}$ ratio to 2.10:8.15. This should, again in theory, have yielded an average metal oxidation state of ca. +3 but instead gave us desired complex **2**. We make no attempt at this time to rationalize the nature of products obtained as a function of reagent ratios, because we feel these reaction systems are too complicated.

Complex **4** represents the first example of a $Mn_3O$ complex with benzoate ligation. Similarly, use of imidazole leads to

(16) Chisholm, M. H.; Folting, K.; Huffman, J. C.; Kirkpatrick, C. C. *Inorg. Chem.* **1984**, *23*, 1021.
(17) Chandler, J. P. *Quantum Chemistry Program Exchange*, Program 66, Indiana University, Bloomington, IN.
(18) Uemura, S.; Spencer, A.; Wilkinson, G. *J. Chem. Soc., Dalton Trans.* **1973**, 2565.
(19) Hessel, L. W.; Romers, C. *Recl. Trav. Chim. Pay-Bas* **1969**, *88*, 545.
(20) Johnson, M. K.; Powell, D. B.; Cannon, R. D. *Spectrochim. Acta* **1981**, *37A*, 995.

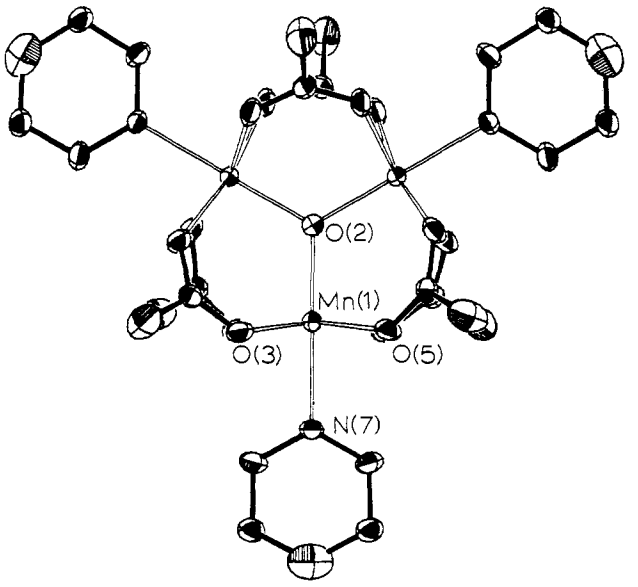


**Figure 1.** ORTEP projection of $Mn_3O(O_2CMe)_6(pyr)_3$ (**2**). The methyl carbon is C(6) and is bound to C(4). Pyridine carbon atoms are numbered consecutively from N(7).

complex **5**, of interest because of the potential importance of manganese-imidazole ligation in biological systems;[1,21] no examples of oxo-bridged manganese–imidazole complexes were known at the outset of our studies. Complexes **2** and **4** have been subjected to a single-crystal X-ray crystallographic analysis. Attempts to obtain suitable crystals of complex **5** have so far been unsuccessful, and continuing work with imidazole-ligated complexes will be presented in a future report.[22]

Complex **2** crystallizes in rhombohedral space group R32. An ORTEP projection is shown in Figure 1. Fractional coordinates and isotropic thermal parameters are listed in Table II; selected bond lengths and angles are listed in Table IV. The crystallographic $C_3$ axis is perpendicular to the $Mn_3$ plane and passes through central oxygen O(2). The overall complex has imposed $32(D_3)$ symmetry so that $Mn_3$ is an equilateral triangle and O(2) and N(7) lie exactly in the $Mn_3$ plane. The Mn coordination geometry is slightly distorted octahedral with four oxygen atoms from bridging acetate groups and a terminal pyridine nitrogen atom completing coordination to each metal. The overall structure is thus of the common "basic carboxylate" type seen for many transition metals.[23,24] The charge on the complex necessitates a mixed-valence $Mn_2^{III}Mn^{II}$ description, but the metals are obviously crystallographically equivalent indicating either rapid *intra*molecular electron transfer or electronic delocalization (vide infra). In the crystal the units stack along the $C_3$ axis with their $Mn_3O$ planes perpendicular to the $C_3$ axes and separated by the solvate pyridine molecules which lie on and are disordered about the $C_3$ axis as described earlier.

The low-temperature structure of complex **2** obtained in this work is essentially identical with the room temperature structure communicated briefly elsewhere.[8] The Mn···Mn (3.363 (1) Å) and Mn–$\mu_3$–O (1.941 (1) Å) distances of the earlier structure compare reasonably with corresponding values in Table IV. Other structural details and the position of the solvate molecules were not reported in the previous work.

Complex **4** crystallizes in monoclinic space group $P2_1$ and contains two independent $Mn_3O$ units in the asymmetric unit. This

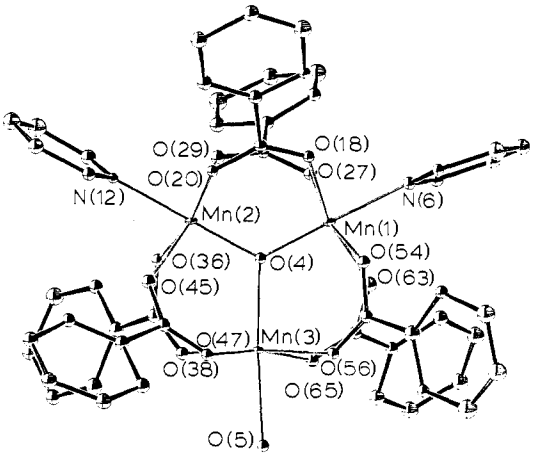


**Figure 2.** ORTEP projection of $[Mn_3O(O_2CPh)_6(pyr)_2(H_2O)]$ (**4**). Carbon atoms are numbered consecutively between O atoms and around aromatic rings.

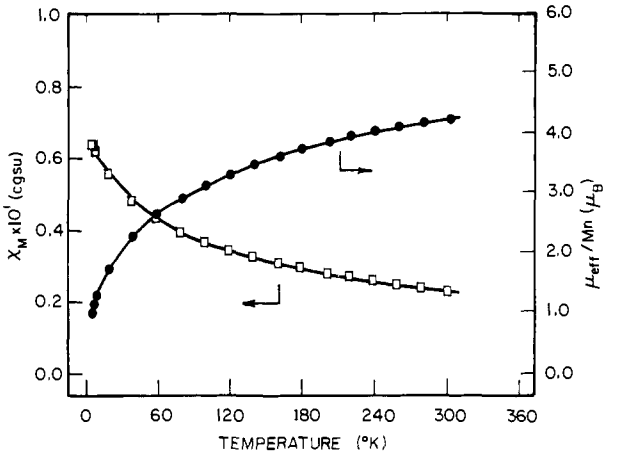


**Figure 3.** Plots of effective magnetic moment per Mn ion, $\mu_{eff}$/Mn, and molar paramagnetic susceptibility, $\chi_m$, vs. temperature for $[Mn_3O(O_2CMe)_6(pyr)_3](ClO_4)$, **1**. The solid lines represent a least-squares fit of the data to the theoretical eq 3.

sample, grown slowly for a structure determination, also contained three MeCN solvate molecules in the asymmetric unit, whereas the analytical sample contained only one MeCN per two $Mn_3O$ units. It was evident at the onset, from the analytical data, that there was something unusual about the formulation of **4**, for it seemed to possess a pyr:Mn ratio of less than unity. The structure determination was therefore carried out and indeed confirmed that **4** is an unusual mixed-ligand species with Mn(3) containing a terminal $H_2O$ group, O(5). An ORTEP projection is shown in Figure 2. Fractional coordinates and isotropic thermal parameters are listed in Table III; selected bond lengths and angles are listed in Table V. The complex again possesses distorted octahedral metal geometries and an overall "basic carboxylate" structure. The molecule approximates to $C_{2v}$ symmetry but has no imposed elements. Central oxygen O(4) lies slightly above the $Mn_3$ plane (0.006 and 0.018 Å in molecules A and B, respectively). The metric parameters of the two molecules are compared in Table V and show little difference. As for **2**, charge consideration necessitates a mixed-valence $Mn_2^{III}Mn^{II}$ description, but the mixed-ligand nature of **4** rationalizes the trapped-valence situation observed in this case. Mn(3) is readily assigned as the $Mn^{II}$ center since Mn(3)–O distances are noticeably longer than those for Mn(1) and Mn(2) as expected for the lower oxidation state. This asymmetry is most noticeable in the $Mn_3O$ central core with the long Mn(3)–O(4) distance leading to the $Mn_3$ triangle being essentially isosceles rather than equilateral; Mn···Mn distances are included in Table V. The Mn(1)···Mn(2) distances (3.214, 3.218 Å) are significantly shorter than the Mn(1,2)···Mn(3) distances (3.350–3.418 Å). The average Mn···Mn separation,

(21) (a) Stallings, W. C.; Pattridge, K. A.; Strong, R. K.; Ludwig, M. L. *J. Biol. Chem.* **1985**, *260*, 16424. (b) Fujimoto, S.; Murakami, K.; Ohara, A. *J. Biochem.* **1985**, *97*, 1777. (c) Padhye, S.; Kambara, T.; Hendrickson, D. N.; Govindjee *Photosynthesis Res.* **1986**, *9*, 103.

(22) Vincent, J. B.; Christmas, C.; Christou, G., work in progress.

(23) Catterick, J.; Thornton, P. *Adv. Inorg. Chem. Radiochem.* **1977**, *20*, 291.

(24) Cotton, F. A.; Wilkinson, G. *Advanced Inorganic Chemistry*, 4th ed.; Wiley: New York, 1980; 154.

**Table III.** Fractional Coordinates and Isotropic Thermal Parameters for **4**[a]

| atom | x | y | z | $B_{iso}$ | atom | x | y | z | $B_{iso}$ |
|---|---|---|---|---|---|---|---|---|---|
| Mn(1) | 9891 (2) | 132[b] | 201 (2) | 19 | N(6)′ | 4192 (11) | −1161 (8) | −5455 (11) | 21 (4) |
| Mn(2) | 10070 (2) | −1180 (2) | −357 (2) | 18 | C(7)′ | 4645 (16) | −1607 (11) | −5642 (16) | 28 (5) |
| Mn(3) | 8104 (2) | −522 (2) | −792 (2) | 20 | C(8)′ | 4380 (18) | −2036 (12) | −6238 (19) | 41 (6) |
| O(4) | 9448 (8) | −520 (6) | −275 (9) | 16 (3) | C(9)′ | 3580 (18) | −1955 (13) | −6746 (19) | 41 (6) |
| O(5) | 6748 (8) | −438 (6) | −1423 (9) | 18 (3) | C(10)′ | 3051 (17) | −1485 (12) | −6545 (17) | 35 (6) |
| N(6) | 10354 (11) | 875 (8) | 782 (11) | 21 (3) | C(11)′ | 3365 (18) | −1061 (13) | −5930 (19) | 44 (7) |
| C(7) | 10780 (13) | 1258 (9) | 258 (13) | 18 (4) | N(12)′ | 4002 (10) | 1657 (7) | −4379 (11) | 14 (3) |
| C(8) | 11015 (16) | 1811 (11) | 579 (17) | 37 (5) | C(13)′ | 3991 (15) | 1959 (11) | −5132 (16) | 25 (5) |
| C(9) | 10768 (15) | 1941 (11) | 1442 (16) | 33 (5) | C(14)′ | 3610 (14) | 2493 (10) | −5191 (15) | 19 (5) |
| C(10) | 10340 (15) | 1552 (11) | 1977 (16) | 32 (5) | C(15)′ | 3223 (16) | 2705 (11) | −4389 (18) | 30 (5) |
| C(11) | 10131 (14) | 1027 (10) | 1592 (15) | 25 (4) | C(16)′ | 3226 (16) | 2402 (12) | −3586 (17) | 33 (6) |
| N(12) | 10808 (10) | −1931 (7) | −482 (10) | 13 (3) | C(17)′ | 3655 (13) | 1852 (9) | −3630 (14) | 16 (4) |
| C(13) | 11161 (14) | −2047 (9) | −1293 (14) | 22 (4) | O(18)′ | 4417 (10) | −76 (7) | −6028 (10) | 26 (3) |
| C(14) | 11653 (15) | −2556 (11) | −1401 (16) | 31 (5) | C(19)′ | 4009 (14) | 366 (10) | −6141 (15) | 17 (4) |
| C(15) | 11785 (17) | −2904 (12) | −634 (18) | 41 (6) | O(20)′ | 3986 (10) | 781 (7) | −5642 (10) | 25 (3) |
| C(16) | 11397 (18) | −2775 (12) | 178 (19) | 46 (6) | C(21)′ | 3522 (14) | 394 (10) | −7069 (15) | 20 (5) |
| C(17) | 10915 (15) | −2270 (10) | 181 (16) | 29 (5) | C(22)′ | 3534 (15) | −52 (10) | −7616 (16) | 25 (5) |
| O(18) | 11186 (8) | 48 (6) | −338 (9) | 17 (3) | C(23)′ | 3047 (17) | −5 (12) | −8453 (19) | 39 (6) |
| C(19) | 11493 (13) | −372 (9) | −730 (14) | 21 (4) | C(24)′ | 2645 (17) | 511 (12) | −8647 (18) | 37 (6) |
| O(20) | 11122 (8) | −844 (6) | −912 (8) | 16 (3) | C(25)′ | 2624 (18) | 949 (13) | −8091 (19) | 43 (6) |
| C(21) | 12452 (14) | −331 (9) | −1118 (15) | 25 (4) | C(26)′ | 3076 (14) | 922 (10) | −7275 (15) | 22 (5) |
| C(22) | 12870 (12) | 184 (9) | −1105 (13) | 17 (4) | O(27)′ | 3483 (9) | −297 (6) | −4366 (10) | 22 (3) |
| C(23) | 13727 (16) | 248 (11) | −1447 (17) | 40 (6) | C(28)′ | 3172 (13) | 94 (10) | −3933 (15) | 19 (4) |
| C(24) | 14119 (15) | −209 (11) | −1850 (16) | 33 (5) | O(29)′ | 3551 (9) | 570 (7) | −3804 (10) | 22 (3) |
| C(25) | 13672 (16) | −742 (11) | −1905 (17) | 35 (5) | C(30)′ | 2273 (14) | 12 (10) | −3520 (15) | 21 (5) |
| C(26) | 12824 (15) | −774 (11) | −1516 (16) | 31 (5) | C(31)′ | 1871 (15) | −554 (11) | −3613 (16) | 32 (5) |
| O(27) | 10282 (9) | −207 (6) | 1362 (9) | 22 (3) | C(32)′ | 997 (18) | −612 (12) | −3169 (19) | 43 (6) |
| C(28) | 10564 (13) | −702 (9) | 1559 (14) | 19 (4) | C(33)′ | 600 (16) | −168 (11) | −2770 (17) | 30 (5) |
| O(29) | 10684 (9) | −1073 (6) | 952 (9) | 26 (3) | C(34)′ | 1003 (15) | 359 (10) | −2737 (16) | 26 (5) |
| C(30) | 10714 (14) | −794 (10) | 2511 (14) | 24 (4) | C(35)′ | 1854 (18) | 469 (12) | −3119 (18) | 38 (6) |
| C(31) | 11003 (13) | −381 (9) | 3071 (14) | 22 (4) | O(36)′ | 5133 (9) | 1128 (6) | −3046 (9) | 19 (3) |
| C(32) | 11031 (16) | −481 (13) | 3996 (18) | 43 (6) | C(37)′ | 5618 (12) | 952 (9) | −2385 (13) | 12 (4) |
| C(33) | 10835 (16) | −1012 (11) | 4337 (17) | 38 (5) | O(38)′ | 6035 (9) | 480 (6) | −2422 (9) | 20 (3) |
| C(34) | 10618 (17) | −1462 (12) | 3753 (18) | 44 (6) | C(39)′ | 5681 (14) | 1302 (10) | −1561 (15) | 22 (5) |
| C(35) | 10562 (15) | −1343 (10) | 2805 (16) | 30 (5) | C(40)′ | 5883 (16) | 1053 (11) | −743 (17) | 30 (5) |
| O(36) | 9188 (9) | −1640 (6) | 249 (9) | 22 (3) | C(41)′ | 5954 (17) | 1419 (12) | 60 (18) | 37 (6) |
| C(37) | 8297 (14) | −1694 (10) | 166 (15) | 26 (5) | C(42)′ | 5821 (16) | 2001 (13) | −62 (18) | 38 (6) |
| O(38) | 7853 (9) | −1362 (6) | −317 (9) | 22 (3) | C(43)′ | 5570 (16) | 2217 (11) | −878 (18) | 36 (6) |
| C(39) | 7914 (14) | −2159 (10) | 607 (15) | 27 (5) | C(44)′ | 5498 (14) | 1865 (10) | −1639 (15) | 24 (5) |
| C(40) | 8363 (14) | −2441 (10) | 1273 (15) | 25 (4) | O(45)′ | 5620 (9) | 1287 (6) | −4900 (9) | 21 (3) |
| C(41) | 8038 (16) | −2937 (12) | 1706 (17) | 41 (6) | C(46)′ | 6426 (15) | 1306 (10) | −4627 (16) | 24 (5) |
| C(42) | 7241 (16) | −3168 (11) | 1348 (17) | 36 (5) | O(47)′ | 6815 (9) | 959 (7) | −4146 (10) | 24 (3) |
| C(43) | 6736 (14) | −2868 (10) | 697 (15) | 28 (5) | C(48)′ | 6937 (14) | 1777 (9) | −5033 (14) | 16 (4) |
| C(44) | 7056 (16) | −2386 (11) | 317 (17) | 36 (5) | C(49)′ | 7902 (21) | 1759 (14) | −4905 (21) | 54 (8) |
| O(45) | 9522 (9) | −1447 (6) | −1665 (9) | 24 (3) | C(50)′ | 8403 (20) | 2212 (14) | −5238 (21) | 51 (7) |
| C(46) | 9016 (13) | −1235 (9) | −2246 (14) | 22 (4) | C(51)′ | 8022 (19) | 2641 (13) | −5708 (20) | 47 (7) |
| O(47) | 8496 (9) | −828 (6) | −2128 (9) | 19 (3) | C(52)′ | 7068 (18) | 2677 (12) | −5803 (19) | 41 (6) |
| C(48) | 9043 (14) | −1529 (10) | −3161 (15) | 26 (4) | C(53)′ | 6582 (16) | 2222 (11) | −5473 (17) | 33 (6) |
| C(49) | 8600 (15) | −1238 (10) | −3910 (15) | 30 (5) | O(54)′ | 5939 (10) | −710 (7) | −5403 (10) | 26 (3) |
| C(50) | 8635 (15) | −1513 (10) | −4733 (16) | 32 (5) | C(55)′ | 6683 (11) | −496 (9) | −5484 (12) | 8 (3) |
| C(51) | 9005 (15) | −2038 (11) | −4839 (16) | 32 (5) | O(56)′ | 7047 (9) | −172 (7) | −4909 (10) | 24 (3) |
| C(52) | 9407 (15) | −2312 (10) | −4091 (16) | 31 (5) | C(57)′ | 7149 (13) | −631 (9) | −6291 (14) | 16 (4) |
| C(53) | 9427 (14) | −2049 (10) | −3236 (14) | 25 (4) | C(58)′ | 7989 (15) | −384 (11) | −6467 (16) | 27 (5) |
| O(54) | 9628 (9) | 617 (6) | −873 (10) | 21 (3) | C(59)′ | 8484 (14) | −506 (11) | −7243 (16) | 25 (5) |
| C(55) | 8881 (14) | 688 (10) | −1319 (15) | 21 (5) | C(60)′ | 8144 (16) | −889 (11) | −7827 (17) | 30 (5) |
| O(56) | 8267 (9) | 331 (6) | −1359 (9) | 17 (3) | C(61)′ | 7307 (16) | −1163 (12) | −7712 (17) | 35 (5) |
| C(57) | 8794 (16) | 1217 (11) | −1811 (17) | 32 (5) | C(62)′ | 6829 (14) | −1012 (10) | −6922 (15) | 24 (5) |
| C(58) | 7965 (14) | 1346 (10) | −2188 (15) | 21 (5) | O(63)′ | 5000 (10) | −1026 (7) | −3793 (10) | 28 (3) |
| C(59) | 7839 (19) | 1853 (13) | −2630 (20) | 50 (7) | C(64)′ | 5655 (14) | −1107 (10) | −3305 (15) | 23 (5) |
| C(60) | 8533 (19) | 2210 (13) | −2836 (19) | 45 (7) | O(65)′ | 6264 (9) | −722 (6) | −3157 (10) | 24 (3) |
| C(61) | 9386 (18) | 2081 (13) | −2487 (19) | 43 (6) | C(66)′ | 5755 (14) | −1637 (10) | −2820 (15) | 21 (5) |
| C(62) | 9548 (15) | 1572 (10) | −1999 (15) | 21 (5) | C(67)′ | 5047 (15) | −2061 (11) | −2890 (16) | 26 (5) |
| O(63) | 8661 (10) | 415 (7) | 780 (10) | 29 (3) | C(68)′ | 5131 (19) | −2572 (13) | −2497 (19) | 46 (7) |
| C(64) | 7837 (14) | 229 (10) | 833 (15) | 22 (5) | C(69)′ | 6006 (20) | −2729 (14) | −2052 (21) | 53 (7) |
| O(65) | 7538 (9) | −154 (7) | 346 (10) | 23 (3) | C(70)′ | 6680 (18) | −2334 (12) | −2071 (19) | 40 (6) |
| C(66) | 7309 (14) | 475 (10) | 1571 (15) | 22 (5) | C(71)′ | 6595 (15) | −1808 (10) | −2419 (16) | 25 (5) |
| C(67) | 7662 (15) | 913 (11) | 2044 (16) | 29 (5) | C(1)A | 9235 (21) | 431 (14) | 5393 (22) | 57 (8) |
| C(68) | 7135 (18) | 1149 (12) | 2754 (18) | 41 (6) | C(2)A | 9484 (20) | 747 (14) | 4596 (22) | 47 (7) |
| C(69) | 6286 (16) | 925 (12) | 2941 (17) | 37 (6) | N(3)A | 9721 (16) | 952 (12) | 3966 (18) | 54 (6) |
| C(70) | 5980 (17) | 483 (12) | 2431 (18) | 37 (6) | C(1)B | 5554 (26) | −954 (18) | 10041 (28) | 74 (10) |
| C(71) | 6445 (16) | 266 (11) | 1696 (17) | 32 (5) | C(2)B | 5150 (34) | −1119 (24) | 10805 (40) | 112 (15) |
| Mn(1)′ | 4751 (2) | −466 (2) | −4843 (2) | 21 | N(3)B | 4895 (29) | −1302 (20) | 11518 (32) | 129 (14) |
| Mn(2)′ | 4640 (2) | 855 (2) | −4335 (2) | 20 | C(1)C | 1798 (25) | 1263 (17) | 4653 (27) | 76 (10) |
| Mn(3)′ | 6465 (2) | 112 (2) | −3713 (2) | 21 | C(2)C | 1354 (31) | 1486 (20) | 5438 (33) | 89 (12) |
| O(4)′ | 5193 (8) | 166 (7) | −4331 (9) | 17 (3) | N(3)C | 970 (29) | 1699 (19) | 5990 (30) | 126 (13) |
| O(5)′ | 7812 (9) | 52 (7) | −3075 (10) | 25 (3) | | | | | |

[a] Fractional coordinates are $\times 10^4$; $B_{iso}$ values are $\times 10$. Primed and unprimed atoms refer to molecules A and B, respectively. The A, B, and C suffixes refer to the three MeCN molecules. [b] Parameters were not varied.

Table IV. Selected Bond Lengths (Å) and Angles (deg) for **2**

| | | | |
|---|---|---|---|
| (a) Bonds | | | |
| Mn···Mn | 3.353 (1) | Mn–O(2) | 1.936 (2) |
| Mn–O(3) | 2.144 (6) | Mn–N(7) | 2.167 (10) |
| Mn–O(5) | 2.066 (7) | | |
| (b) Angles | | | |
| O(2)–Mn–O(3) | 94.60 (16) | O(2)–Mn–N(7) | 180.00 |
| O(2)–Mn–O(5) | 95.74 (18) | O(3)–Mn–N(7) | 85.40 (18) |
| O(3)–Mn–O(5) | 89.80 (30) | O(5)–Mn–N(7) | 84.26 (21) |
| O(3)–Mn–O(3)′ | 170.81 (18) | O(5)–Mn–O(5)′ | 168.52 (21) |
| Mn–O(2)–Mn | 120.00 | | |

Table V. Selected Bond Lengths (Å) and Angles (deg) for **4**

| parameter | molecule A | molecule B |
|---|---|---|
| Mn(1)···Mn(2) | 3.218 (4) | 3.214 (6) |
| Mn(1)···Mn(3) | 3.418 (5) | 3.350 (5) |
| Mn(2)···Mn(3) | 3.396 (5) | 3.376 (5) |
| Mn(1)–O(4) | 1.817 (14) | 1.798 (15) |
| Mn(2)–O(4) | 1.822 (14) | 1.827 (15) |
| Mn(3)–O(4) | 2.154 (13) | 2.116 (13) |
| Mn(1)–O(18) | 2.132 (13) | 2.051 (16) |
| Mn(1)–O(27) | 1.992 (15) | 2.090 (15) |
| Mn(1)–O(54) | 2.006 (15) | 2.070 (16) |
| Mn(1)–O(63) | 2.164 (16) | 2.083 (16) |
| Mn(1)–N(6) | 2.074 (19) | 2.052 (19) |
| Mn(2)–O(20) | 1.968 (14) | 2.181 (16) |
| Mn(2)–O(29) | 2.166 (15) | 1.955 (15) |
| Mn(2)–O(36) | 1.952 (15) | 2.152 (15) |
| Mn(2)–O(45) | 2.202 (15) | 1.993 (15) |
| Mn(2)–N(12) | 2.103 (17) | 2.123 (18) |
| Mn(3)–O(5) | 2.244 (13) | 2.230 (14) |
| Mn(3)–O(38) | 2.143 (15) | 2.223 (15) |
| Mn(3)–O(47) | 2.216 (15) | 2.169 (16) |
| Mn(3)–O(56) | 2.199 (14) | 2.115 (16) |
| Mn(3)–O(65) | 2.105 (15) | 2.159 (16) |
| Mn(2)–Mn(1)–Mn(3) | 61.47 (9) | 61.88 (11) |
| Mn(1)–Mn(2)–Mn(3) | 62.17 (10) | 61.05 (11) |
| Mn(1)–Mn(3)–Mn(2) | 56.36 (9) | 57.08 (11) |
| O(4)–Mn(1)–N(6) | 177.6 (6) | 176.9 (7) |
| O(4)–Mn(2)–N(12) | 178.4 (7) | 178.4 (7) |
| O(4)–Mn(3)–O(5) | 173.5 (6) | 179.4 (6) |
| O(4)–Mn(1)–O(18,27,54,63)[a] | 96.05 | 94.83 |
| N(6)–Mn(1)–O(18,27,54,63)[a] | 84.03 | 85.13 |
| O(4)–Mn(2)–O(20,29,36,45)[a] | 95.20 | 96.32 |
| N(12)–Mn(2)–O(20,29,36,45)[a] | 84.85 | 83.73 |
| O(4)–Mn(3)–O(38,47,56,65)[a] | 93.45 | 93.53 |
| O(5)–Mn(3)–O(38,47,56,65)[a] | 83.90 | 86.53 |

[a] Average of four values.

however, (3.329 Å) is quite similar to that seen in the electronically delocalized complex **2** (3.353 Å). In **2**, the pyridine rings are essentially coplanar with the $Mn_3$ plane, but in **4** they are almost perpendicular, probably due to greater steric interactions with the benzoate groups.

**Magnetic Susceptibility Data for $Mn_3^{III}O$ Complex 1.** Variable temperature (~6 to ~340 K) magnetic susceptibility data were collected for microcrystalline samples of compounds **1–4**. These data, in conjunction with the calculated susceptibility values resulting from the least-squares fit to the appropriate equations (vide infra), are compiled in Tables IS, IIS, IIIS, IVS, and VS[25] (Supplementary Material).

All of the manganese ions in $[Mn_3O(O_2CMe)_6(pyr)_3](ClO_4)$, **1**, are of the same valence. As can be seen in Figure 3, the value of $\mu_{eff}$/Mn for **1** gradually varies from 4.25 $\mu_B$ at 302.16 K to 1.01 $\mu_B$ at 5.99 K. The effective magnetic moment per manganese ion at 302.16 K is somewhat less than would be expected for the spin-only value associated with a high-spin $d^4$ ion, namely 4.90 $\mu_B$ for four unpaired electrons ($S = 2$); however, it clearly exceeds the 2.83 $\mu_B$ value expected for a low-spin $Mn^{III}$ ion with $S = 1$. Thus, it is clear that **1** contains high-spin $Mn^{III}$ ions. Furthermore, from the data in Figure 3, it is also clear that the intramolecular magnetic exchange interaction in **1** is weak.

The spin Hamiltonian which describes the isotropic magnetic exchange interaction in a triangulated trinuclear complex is given in eq 2. In compound **1**, $S_1 = S_2 = S_3 = 2$, and if all three $Mn^{III}$ ions are equivalent $J_{12} = J_{23} = J_{31} = J$. The molar paramagnetic susceptibility for such a trinuclear complex is given below. In eq 3 $x = J/kT$, $g$ is the average $g$ value, and the other symbols have their usual meanings. The ground state for a $Mn_3^{III}O$ complex is characterized by a total spin of $S' = S_1 + S_2 + S_3 = 0$ with $S^* = S_1 + S_3 = 2$.

$$\hat{H} = -2[J_{12}(\hat{S}_1\cdot\hat{S}_2) + J_{23}(\hat{S}_2\cdot\hat{S}_3) + J_{31}(\hat{S}_3\cdot\hat{S}_1)] \quad (2)$$

$$X_M = \frac{Ng^2\beta^2}{3kT} \times \left[\frac{546e^{42x} + 660e^{30x} + 540e^{20x} + 336e^{12x} + 150e^{6x} + 18e^{2x}}{13e^{42x} + 22e^{30x} + 27e^{20x} + 28e^{12x} + 25e^{6x} + 9e^{2x} + 1}\right] \quad (3)$$

The paramagnetic susceptibility data for **1** were least-squares fit to eq 3 to give the fitting parameters $J = -10.2$ cm$^{-1}$ and $g = 1.81$. The solid line in Figure 3 represents this fit. In this type of $\mu_3$-oxo-bridged trinuclear complex, it is very likely that the majority of this interaction is propagated by the oxide bridge, not by the acetate bridges. The Mn–O–Mn angles in **1** should be close to 120°. Unfortunately, there are not very many well-characterized oxo-bridged binuclear or trinuclear $Mn^{III}$ complexes with which to compare the properties of **1**.

Wieghardt et al.[26] very recently reported the synthesis and X-ray structures for two binuclear $Mn^{III}$ complexes, both possessing $\mu$-oxo, bis($\mu$-carboxylato) bridging units. The Mn–O–Mn angles in these two complexes were found to be 117.9 (2) and 120.9 (1)°. It was reported that in the 120–298 K range, the magnetic susceptibilities of powdered samples of these two complexes adhere closely to the Curie–Weiss law. Thus, the *intra*molecular magnetic exchange interactions in these two complexes are quite weak. Torihara et al.[27] recently reported several binuclear $Mn^{III}$ complexes where two alkoxide oxygen atoms serve as the bridge between the two $Mn^{III}$ ions. The X-ray structure of one of these complexes was described, and the bridging angle in the $Mn_2(\mu\text{-}OR)_2$ moiety was reported as 96.34 (8)°. Antiferromagnetic exchange interactions with $J$ values in the range of −13.5 to −20.4 cm$^{-1}$ were found for these binuclear Schiff-base complexes. Finally, it is somewhat relevant to note that a $J$ value of −150 cm$^{-1}$ has been reported[28] for the $Mn^{III}Mn^{IV}$ mixed-valence $\mu_2$-oxo compound $[(bipy)_2MnO_2Mn(bipy)_2](ClO_4)_3\cdot 2H_2O$, where bipy is 2,2′-bipyridine. The value of the Mn–O–Mn angle in this complex has not been reported, for the X-ray structure has only been communicated.[29]

Considerable effort has been expended to understand the temperature dependence of the magnetic susceptibility data for various $\mu_3$-oxo-bridged trinuclear $Fe^{III}$ acetate complexes. In general, the susceptibility vs. temperature curves are *not* fit well by the intracluster isotropic exchange Hamiltonian, eq 2, used in the above analysis of the data for the $Mn_3^{III}O$ compound **1**. A variety of theoretical magnetic exchange models involving nonequivalent coupling constants,[30] intercluster exchange,[31] biquadratic exchange,[32] dynamic distortion,[33] and monomeric impurities have

(25) See Supplementary Material.

(26) Wieghardt, K.; Bossek, U.; Ventur, D.; Weiss, J. *J. Chem. Soc., Chem. Commun.* **1985**, 347.

(27) (a) Torihara, N.; Mikuriya, M.; Okawa, H.; Kida, S. *Bull. Chem. Soc. Jpn.* **1980**, *53*, 1610. (b) Mikuriya, M.; Torihara, N.; Okawa, H.; Kida, S. *Bull. Chem. Soc. Jpn.* **1981**, *54*, 1063.

(28) Cooper, S. R.; Dismukes, G. C.; Klein, M. P.; Calvin, M. *J. Am. Chem. Soc.* **1978**, *100*, 7248.

(29) Plaksin, P. M.; Stoufer, R. C.; Mathew, M.; Palenik, G. J. *J. Am. Chem. Soc.* **1972**, *94*, 2121.

(30) (a) Wucher, J.; Gijsman, H. M. *Physica* **1954**, *20*, 361. (b) Kambe, K. *J. Phys. Soc. Jpn.* **1950**, *48*, 5.

(31) (a) Dziobkowski, C. T.; Wrobleski, J. T.; Brown, D. B. *Inorg. Chem.* **1981**, *20*, 671. (b) Tsukerblat, B. S.; Belinskii, M. I.; Kuyavskaya, B. Ya. *Inorg. Chem.* **1983**, *22*, 995. (c) Güdel, H. U. *J. Chem. Phys.* **1985**, *82*, 2510.

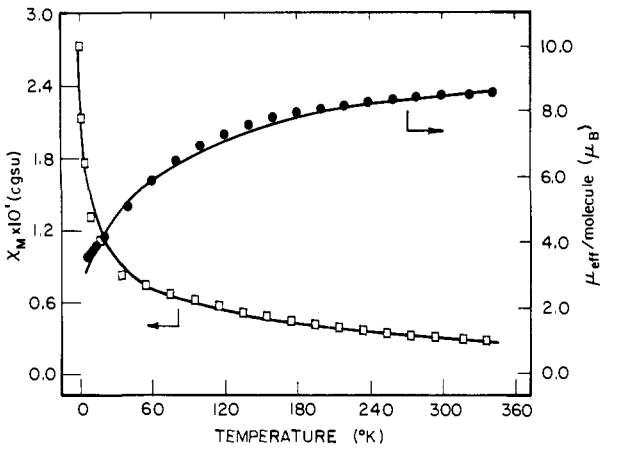


**Figure 4.** Plots of effective magnetic moment ($\mu_{eff}$) per $Mn_3O$ molecule and molar paramagnetic susceptibility, $\chi_m$, vs. temperature for $[Mn_3O(O_2CMe)_6(pyr)_3](pyr)$ (**2**). The solid lines represent a least-squares fit of the data to the theoretical eq 4.

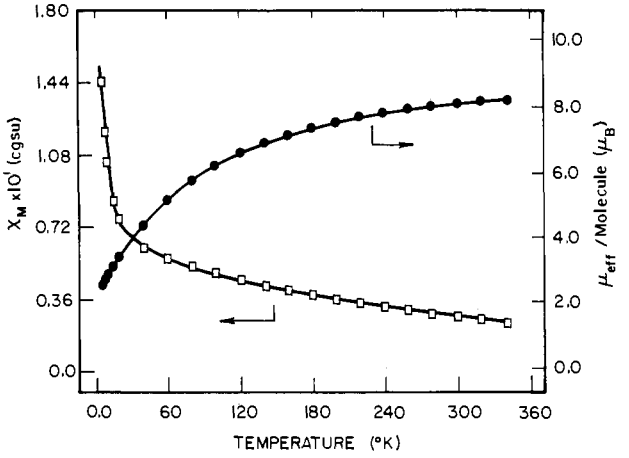


**Figure 5.** Plots of effective magnetic moment ($\mu_{eff}$) per $Mn_3O$ molecule and molar paramagnetic susceptibility, $\chi_m$, vs. temperature for $[Mn_3O(O_2CMe)_6(pyr)_3]$ (**3**). The solid lines represent a least-squares fit of the data to the theoretical eq 4.

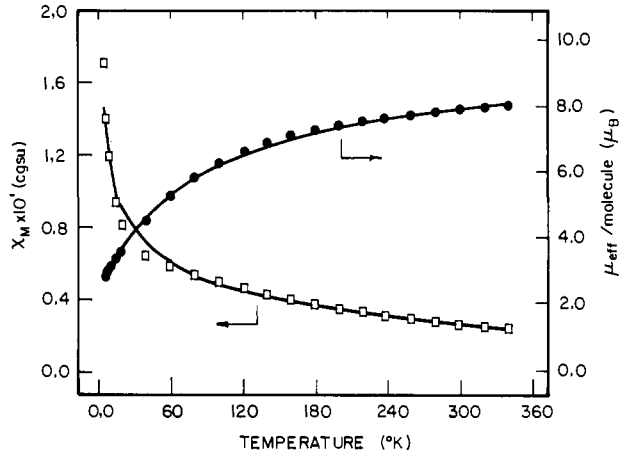


**Figure 6.** Plots of effective magnetic moment ($\mu_{eff}$) per $Mn_3O$ molecule and molar paramagnetic susceptibility, $\chi_m$, vs. temperature for $[Mn_3O(O_2CPh)_6(pyr)_2(H_2O)]\cdot 0.5$ MeCN (**4**). The solid lines represent a least-squares fit of the data to the theoretical eq 4.

been proposed for the $Fe_3^{III}O$ complexes. Regardless of the details of the data fitting, the $J$ values for these $Fe_3^{III}O$ complexes fall in the approximate range of $-23$ to $-31$ $cm^{-1}$.

It seems that the antiferromagnetic exchange interaction increases in going from the $Mn_3^{III}O$ to the $Fe_3^{III}O$ acetate complexes. This can be rationalized by noting that the $Mn^{III}$ ion is a high-spin $d^4$ ion with the (octahedral) electron configuration of $t_{2g}^3e_g$ whereas the $Fe^{III}$ ion is high-spin $d^5$ with $t_{2g}^3e_g^2$. Unpaired electrons in the $e_g$ orbitals contribute antiferromagnetic exchange pathways, because the $e_g$ orbitals are involved in $\sigma$ interactions. The decreasing antiferromagnetic exchange interaction in the order NiO > CoO > FeO > MnO for this series of rock-salt structure oxides has been rationalized in this manner.[34] Also, in two series of complexes of the composition $LM_2^{II}X_2$, where L is a binucleating ligand and X = $Cl^-$, the antiferromagnetic exchange interaction was reported[35,36] to decrease as the number of unpaired electrons increased in the series. Another possible explanation for the weaker antiferromagnetic interaction in the $Mn_3^{III}O$ complexes compared to the $Fe_3^{III}O$ complexes is that it is due to the short $Mn^{III}$–O(oxide) bond length. The two independent $Mn_3O$ units in valence-localized complex **4** have $Mn^{III}$–O(oxide) distances in the range 1.798–1.827 Å which is to be compared with the $Mn^{II}$–O(oxide) distances of 2.116 and 2.154 Å in **4**. The short $Mn^{III}$–O(oxide) distance could raise the energy of the $d_{z^2}$ orbital directed along the $Mn^{III}$–O(oxide) bond vector. This highest energy d-orbital is, therefore, empty in the high-spin $d^4$ $Mn^{III}$ ion, a situation reflected in the relatively short $Mn^{III}$–N(pyr) distances. In high-spin $Fe^{III}$, the corresponding $d_{z^2}$ orbital is partially occupied. This difference could contribute to an increased antiferromagnetic exchange interaction for the $Fe_3^{III}O$ complexes compared to the $Mn_3^{III}O$ complexes.

**Magnetic Susceptibility Data for the Mixed-Valence $Mn_2^{III}Mn^{II}O$ Complexes.** The magnetochemistry of the three mixed-valence complexes **2**, **3**, and **4** was examined. In Figures 4, 5, and 6 are given plots of the effective magnetic moment *per molecule* ($\mu_{eff}$/molecule) vs. temperature. The value of $\mu_{eff}$/molecule gradually decreases from 8.58 $\mu_B$ at 342.01 K to 3.61 $\mu_B$ at 6.00 K for compound **2**. The properties of compound **3** are very similar: $\mu_{eff}$/molecule varies from 8.24 $\mu_B$ at 342.70 K to 2.63 $\mu_B$ at 6.00 K. A comparison of the magnetochemical properties of these two compounds is particularly interesting, for the rates of electron transfer in the analogous $Fe_3O$ compounds have been studied in great detail.[2-7] $[Fe_3O(O_2CMe)_6(pyr)_3](pyr)$ is isostructural with **2**.[5] There are stacks of $Fe_3O$ complexes with a $C_3$ axis running down the stack above 190 K. Each pyridine solvate molecule is sandwiched between two $Fe_3O$ complexes with the plane of the pyridine solvate molecule parallel to the $C_3$ axis but perpendicular to the $Fe_3O$ planes. $[Fe_3O(O_2CMe)_6(pyr)_3](pyr)$ undergoes essentially two phase transitions,[3] a low-temperature (LT) one at 112 K and a high-temperature (HT) phase transition at 190 K. Mössbauer spectra show that the rate of intramolecular electron transfer begins to increase at 112 K and finally becomes very fast at 190 K.[2] Single-crystal solid-state $^2H$ NMR results[6] have clearly indicated that the pyridine solvate molecules begin to rotate rapidly about the $C_3$ axis at 190 K. On the other hand, the compound $[Fe_3O(O_2CMe)_6(pyr)_3]$, which is prepared by simply recrystallizing the pyridine solvate complex from MeCN, does not show an increase in electron-transfer rate with increasing temperature. It is still valence-trapped at 315 K as clearly indicated by Mössbauer spectroscopy. Thus, it is reasonable to expect that $Mn_3O$ compound **2** experiences an onset of lattice dynamics (i.e., rotation of the pyridine solvate molecules) with increasing temperature, whereas there is no element of the lattice of compound **3** which could become dynamic.

A theoretical expression for the molar paramagnetic susceptibility of a valence-trapped $Mn_2^{III}Mn^{II}O$ complex can be derived, assuming isotropic exchange interactions and by using the spin Hamiltonian in eq 2. If it is assumed that the two $Mn^{III}$ ions are equivalent, then there are two exchange parameters, $J = J_{12} = J_{31}$ for the $Mn^{II}$–$Mn^{III}$ interactions and $J' = J_{23}$ for the $Mn^{III}$–$Mn^{III}$

(32) (a) Uryu, N.; Friedburg, S. A. *Phys. Rev.* **1965**, *A140*, 183. (b) Rakitin, Y. V.; Zhemchuzhnikova, T. A.; Zelentsov, V. V. *Inorg. Chim. Acta* **1977**, *23*, 145.
(33) Jones, D. H.; Sams, J. R.; Thompson, R. C. *J. Chem. Phys.* **1984**, *81*, 440.
(34) (a) Foex, M. C. R. *Hebd. Seances Acad. Sci.* **1948**, *227*, 193. (b) Anderson, P. W. *Phys. Rev.* **1959**, *115*, 2.
(35) Lambert, S. L.; Hendrickson, D. N. *Inorg. Chem.* **1979**, *18*, 2683.
(36) Spiro, C. L.; Lambert, S. L.; Smith, T. S.; Duesler, E. N.; Gagne, R. R.; Hendrickson, D. N. *Inorg. Chem.* **1981**, *20*, 1229.

**Table VI.** Parameters Resulting from Least-Squares Fitting of Magnetic Susceptibility Data

| compound | $J$, cm$^{-1}$ | $J'$, cm$^{-1}$ | $g$ |
|---|---|---|---|
| $[Mn_3O(O_2CMe)_6(pyr)_3](ClO_4)$ (**1**) | −10.2 | | 1.81 |
| $[Mn_3O(O_2CMe)_6(pyr)_3](pyr)$ (**2**) | −5.1 | −8.3 | 2.13 |
| $[Mn_3O(O_2CMe)_6(pyr)_3](pyr)_{0.7}$ (**6**) | −5.6 | −6.4 | 2.07 |
| $[Mn_3O(O_2CMe)_6(pyr)_3]$ (**3**) | −7.7 | −5.7 | 2.10 |
| $[Mn_3O(O_2CPh)_6(pyr)_2(H_2O)]\cdot 0.5MeCN$ (**4**) | −7.3 | −10.9 | 2.11 |

interaction, and the molar paramagnetic susceptibility is given by eq 4. In this expression, $x = J/kT$ and $y = J'/kT$. The ground state for such an $Mn^{II}Mn_2^{III}O$ complex has a total spin of $S' = {}^1/_2$.

$$X_M = \frac{Ng^2\beta^2}{3kT} \times \frac{1}{2}\left[\frac{1365\exp(28x+20y)+858\exp(15x+20y)+858\exp(23x+12y)}{14\exp(28x+20y)+12\exp(15x+20y)+12\exp(23x+12y)} + \frac{495\exp(4x+20y)+495\exp(12x+12y)+495\exp(18x+6y)}{10\exp(4x+20y)+10\exp(12x+12y)+10\exp(18x+6y)} + \frac{252\exp(20y-5x)+252\exp(3x+12y)+252\exp(9x+6y)}{8\exp(20y-5x)+8\exp(3x+12y)+8\exp(9x+6y)} + \frac{252\exp(13x+2y)+105\exp(20y-12x)+105\exp(12y-4x)}{8\exp(13x+2y)+6\exp(20y-12x)+6\exp(12y-4x)} + \frac{105\exp(2x+6y)+105\exp(6x+2y)+105\exp(8x)}{6\exp(2x+6y)+6\exp(6x+2y)+6\exp(8x)} + \frac{30\exp(20y-17x)+30\exp(12y-9x)+30\exp(6y-3x)}{4\exp(20y-17x)+4\exp(12y-9x)+4\exp(6y-3x)} + \frac{30\exp(x+2y)+3\exp(12y-12x)+3\exp(6y-6x)}{4\exp(x+2y)+2\exp(12y-12x)+2\exp(6y-6x)}\right] \quad (4)$$

The magnetic susceptibility data for compounds **2** and **3** are fit reasonably well by eq 4; see Figures 4 and 5. The fitting parameters for **2** are $J = -5.1$ cm$^{-1}$, $J' = -8.3$ cm$^{-1}$, and $g = 2.13$ (see Table VI). For **3**, the fitting parameters are $J = -7.7$ cm$^{-1}$, $J' = -5.7$ cm$^{-1}$, and $g = 2.10$. The exchange parameters for **2** and **3** do not differ appreciably from the −10.2 cm$^{-1}$ value for the exchange parameter of the $Mn_3^{III}O$ compound **1**.

It is hard to say what significance should be attached to the fact that the susceptibilities of **2** and **3** are so similar. Close examination of the data illustrated in Figures 4 and 5 shows that the data for **3** are fit better than the data for **2** throughout the full temperature range. It appears that compared to the case for **3** in the range of 180 to 6 K, there are some systematic deviations of the data for **2** from the least-squares fit line. It is in this temperature region where by analogy to the work on the analogous iron complex the onset of lattice dynamics may occur for **2**. However, the deviations from the theoretical curve do not seem to be appreciable. Single-crystal magnetic susceptibility measurements would have to be made in order to determine the significance of these small deviations in the average susceptibilities.

During the course of this work it was found that samples of **2** could be prepared with less than a full complement of pyridine solvate molecules. In fact, there seems to be some tendency for **2** to lose pyridine solvate molecules. Magnetic susceptibility data were collected for a sample which analyzed as $[Mn_3O(O_2CMe)_6(pyr)_3](pyr)_{0.7}$ (**6**) (the data are available in the Supplementary Material). $\mu_{eff}$/molecule varied from 8.40 $\mu_B$ at 339.72 K to 2.17 $\mu_B$ at 5.99 K for this sample. These data were also fit to eq 4 to give the fitting parameters summarized in Table VI. It is interesting that the $J$ and $J'$ values for this $(pyr)_{0.7}$ solvate are intermediate between those for compounds **2** and **3**.

Finally, susceptibility data were collected for the benzoate mixed-valence complex **4** (data in Supplementary Material). For **4**, $\mu_{eff}$/molecule varies from 8.15 $\mu_B$ at 340.20 K to 2.86 $\mu_B$ at 6.00 K. As indicated above, the $Mn^{II}$ ion has a $H_2O$ ligand, whereas the two $Mn^{III}$ ions each have a pyridine ligand. This compound would clearly have a valence-trapped structure with a very low rate of *intra*molecular electron transfer. It is interesting, but perhaps fortuitous, that the $Mn^{III}$–$Mn^{III}$ interaction in **4** ($J' = -10.9$ cm$^{-1}$) is close in magnitude to the interaction in the $Mn_3^{III}O$ compound **1**.

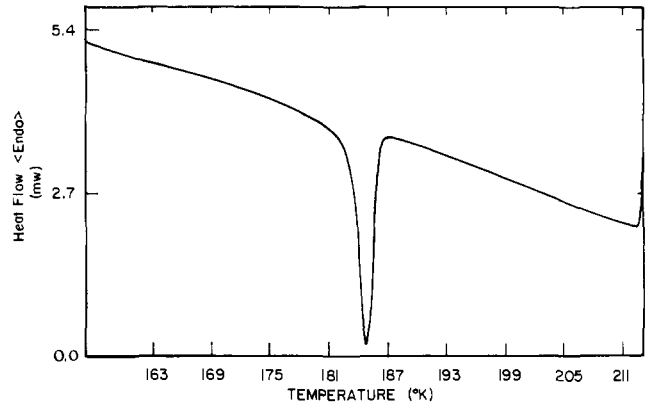


**Figure 7.** The cooling DSC thermogram for a microcrystalline sample of $[Mn_3O(O_2CMe)_6(pyr)_3](pyr)$ (**2**). The scan rate was 5 deg/min.

**Phase Transitions.** In view of the fact that two phase transitions have been characterized by heat capacity measurements[3] for $[Fe_3O(O_2CMe)_6(pyr)_3](pyr)$ at ~112 and ~190 K, it was of interest to see if isostructural compound **2** also shows thermal effects. At the outset, it is important to point out that we have found neither of the other two mixed-valence $Mn_3O$ complexes to show a thermal effect in their DSC thermograms.

In Figure 7 is shown the DSC thermogram obtained for a microcrystalline sample of **2**. A scan range of 153–303 K was employed, which was scanned at rates of 5–10 deg/min. In Figure 7 is shown the thermogram obtained while cooling a freshly prepared microcrystalline sample of **2** from ~213 K down to ~157 K. An exothermic thermal effect is clearly evident with a peak at 184.7 K in the cooling curve. A small hysteresis of ~3 deg was seen in a heating–cooling cycle run at a rate of 10 deg/min. It is interesting that $[Fe_3O(O_2CMe)_6(pyr)_3](pyr)$ exhibits an HT phase transition which actually consists of two maxima in the $C_p$ vs. temperature curve at 185.8 and 191.5 K. The transition at 191.5 K is of higher order; it starts at as low a temperature as ~113 K and culminates at ~192 K. DSC data are not as accurate as those that can be obtained from a heat capacity study. Integration of the area under the peak in Figure 7 gives $\Delta H = 4.56$ kJ/mol. With the critical temperature taken as 184.7 K, this gives a total entropy change of $\Delta S = 24.7$ J/K·mol for this phase transition. This is close to the value of 26.04 J/K·mol obtained in the heat capacity for the HT phase transition in the $Fe_3O$ complex. Clearly, very similar phenomena are involved for the $Mn_3O$ and $Fe_3O$ complexes.

In the case of the $Fe_3O$ complex, the HT phase transition has been associated with both the onset of motion (i.e., rotation about the $C_3$ axis) for the pyridine solvate molecules as well as a conversion of the $Fe_3O$ complex from electronically localized to dynamically delocalized (i.e., fast electron transfer). It is surprising that the $Mn_3O$ complex would have similar electron-transfer characteristics as the $Fe_3O$ complex. This is surprising because the intramolecular magnetic exchange interactions in the mixed-valence $Fe_3O$ complexes are considerably stronger than those in the $Mn_3O$ complex. For example, the susceptibility data for $[Fe_3O(O_2CMe)_6(H_2O)_3]$ have been fit[37] to give $J = -50.0$ cm$^{-1}$ and $J' = -14.5$ cm$^{-1}$. These $J$ values are, of course, larger than those we found for the three mixed-valence $Mn_3O$ complexes. In short, the excited-state potential-energy surfaces for a given $Mn_3O$ complex should be much nearer in energy to the ground-state surface than that found in the analogous $Fe_3O$ complex. The intermetal electronic coupling in the $Mn_3O$ complexes is reduced appreciably compared to the $Fe_3O$ analogue. These facts would have been expected to lead to different electron-transfer characteristics.

(37) Dziobkowski, C. T.; Wrobleski, J. T.; Brown, D. B. *Inorg. Chem.* **1981**, *20*, 679.

The less than totally solvated form of complex **2**, i.e., $[Mn_3O(O_2CMe)_6(pyr)_3](pyr)_{0.7}$ (**6**), did not show a visible thermal effect in its DSC thermogram. It is likely that the defect concentration is appreciably greater in this nonstoichiometric compound **6**. Thermal effects associated with phase transitions could then become broad, eventually becoming so broad that they could not be distinguished from the background.

**Acknowledgment.** Work at Indiana University was supported by NSF Grant CHE-8507748. The diffractometer used by the MSC was funded by NSF Grant CHE-7709496. Partial funding for the research carried out at the University of Illinois was obtained from NIH Grant HL13652.

**Supplementary Material Available:** Complete listings of atomic coordinates, anisotropic thermal parameters, bond distances, and angles for **2** and **4** and magnetic susceptibility data for **1–4** (21 pages); listing of observed and calculated structure factors (13 pages). Ordering information is given on any current masthead page. Complete copies of the MSC Structure Reports (85096 and 86033 for **2** and **4**, respectively) are available on request from the Indiana University Chemistry Library.

# Conformational Analysis for the Pseudooctahedral Complexes $(\eta^5\text{-}C_5H_5)Fe(CO)(PPh_3)CH_2R$ [R = Me, Et, *i*-Pr, *t*-Bu, $SiMe_3$, $(PMe_3)^+$, $(PPh_3)^+$, Mesityl, Ph, Vinyl, 1-Naphthyl]: X-ray Crystal Structures of $(\eta^5\text{-}C_5H_5)Fe(CO)(PPh_3)CH_2R$ (R = Me, $SiMe_3$)

**Stephen G. Davies,* Isabelle M. Dordor-Hedgecock, Kevin H. Sutton, and Mark Whittaker**

*Contribution from the Dyson Perrins Laboratory, Oxford OX1 3QY, U.K.*
*Received March 2, 1987*

**Abstract:** A conformational analysis for the ligands $CH_2R$ attached to the pseudooctahedral chiral auxiliary $[(\eta^5\text{-}C_5H_5)Fe(CO)(PPh_3)]$ is presented. For the complexes $[(\eta^5\text{-}C_5H_5)Fe(CO)(PPh_3)CH_2R]$ (**1**) R = (a) Me, (b) Et, (c) *i*-Pr, (d) *t*-Bu, (e) $SiMe_3$, (f) $[PMe_3]^+$, and (g) $[PPh_3]^+$ $^1H$ NMR spectroscopic analysis, including variable temperature studies, indicates that only one conformation, that where the R group resides in the space between the cyclopentadienyl ligand and the CO ligand with one methylene hydrogen approximately antiperiplanar to the CO ligand, conformation I, is populated. This is confirmed by X-ray crystal structure analyses for the complexes **1a** (R = Me) and **1e** (R = $SiMe_3$) and NOE data for complexes **1d** (R = *t*-Bu), **1e** (R = $SiMe_3$), and **1f** (R = $[PMe_3]^+$). For complex **1h** (R = mesityl) conformation I is unattainable, because of the lateral bulk of the mesityl group, and it adopts a single conformation with R (mesityl) essentially eclipsing the cyclopentadienyl ligand such that a methylene hydrogen is approximately eclipsing the CO ligand, conformation IV. In contrast to the above, complexes **1**, R = (i) Ph, (j) vinyl, and (k) 1-naphthyl, where R is planar, do show significant variation with temperature of their $^3J_{PH}$ coupling constants for both methylene protons consistent with the two conformations I and IV being populated. These results are in complete agreement with a previously proposed theoretically based conformational analysis.

The chiral auxiliary $[(\eta^5\text{-}C_5H_5)Fe(CO)(PPh_3)]$ has been shown to exert powerful stereocontrol in a wide variety of reactions of attached ligands.[1,2] In order to rationalize this remarkable stereocontrol we recently proposed a conformational analysis for complexes of the type $[(\eta^5\text{-}C_5H_5)Fe(CO)(PPh_3)CH_2R]$ based on extended Huckel calculations.[3,4] This analysis, which is at variance with the previous long standing model,[5-10] has come in for considerable criticism,[11,12] although recently it has been successfully employed not only by ourselves[13] but also by others to this same iron system[14] and to rationalize some stereoselective reactions of ligands attached to the analogous rhenium chiral auxiliary $[(\eta^5\text{-}C_5H_5)Re(NO)(PPh_3)]$.[15] We describe here our experimental studies on the conformational properties of the complexes $[(\eta^5\text{-}C_5H_5)Fe(CO)(PPh_3)CH_2R]$ (**1**) where R is (a) Me, (b) Et, (c) *i*-Pr, (d) *t*-Bu, (e) $SiMe_3$, (f) $[PMe_3]^+$, (g) $[PPh_3]^+$, (h) mesityl, (i) Ph, (j) vinyl, and (k) 1-naphthyl.

The new conformational analysis for complexes **1** was based on a pseudooctahedral model which took into account the dominant steric properties of the triphenylphosphine ligand. It predicted that for **1** (R = alkyl) three stable conformations exist with the order of stability I ≫ II > III (Figure 1),[3,4] whereas previously it had been deduced that III > I > II.[5-10] In particular the new model predicted that even for complex **1a** (R = Me) only conformer I (R = Me) would be significantly populated. Criticisms of this model[11,12] have been levied on the basis of the observed

(1) Baird, G. J.; Davies, S. G. *J. Organomet. Chem.* **1983**, *248*, CI. Davies, S. G.; Dordor-Hedgecock, I. M.; Warner, P.; Jones, R. H.; Prout, K. *J. Organomet. Chem.* **1985**, *285*, 213. Liebeskind, L. S.; Welker, M. E. *Tetrahedron Lett.* **1984**, *25*, 4341. Davies, S. G.; Walker, J. C. *J. Chem. Soc., Chem. Commun.* **1985**, 209; **1986**, 495, 609. Davies, S. G.; Easton, R. J. C.; Gonzalez, A.; Preston, S. C.; Sutton, K. H.; Walker, J. C. *Tetrahedron* **1986**, *42*, 3987. Davies, S. G.; Dordor-Hedgecock, I. M.; Sutton, K. H.; Walker, J. C. *Tetrahedron* **1986**, *42*, 5123. Liebeskind, L. S.; Welker, M. E.; Fengl, R. W. *J. Am. Chem. Soc.* **1986**, *108*, 6328.

(2) The iron acetyl complex $(\eta^5\text{-}C_5H_5)Fe(CO)(PPh_3)COCH_3$ is available either as a racemate or enantiomerically pure ((*S*)-(±) and (*R*)-(−) forms) from B. P. Chemicals Ltd., New Specialities Business, Belgrave House, 76 Buckingham Palace Road, London, SW1W OSU, U.K.

(3) Seeman, J. I.; Davies, S. G. *J. Chem. Soc., Chem. Commun.* **1984**, 1019.

(4) Seeman, J. I.; Davies, S. G. *J. Am. Chem. Soc.* **1985**, *107*, 6522.

(5) Thomson, J.; Kenney, W.; Baird, M. C.; Reynolds, W. F. *J. Organomet. Chem.* **1972**, *40*, 205.

(6) Stanley, K.; Zelonka, R. A.; Thomson, J.; Fiess, P.; Baird, M. C. *Can. J. Chem.* **1974**, *52*, 1781.

(7) Stanley, K.; Baird, M. C. *Inorg. Nucl. Chem. Lett.* **1974**, *10*, 1111.

(8) Stanley, K.; Baird, M. C. *J. Am. Chem. Soc.* **1975**, *97*, 4292.

(9) Stanley, K.; Baird, M. C. *J. Am. Chem. Soc.* **1975**, *97*, 6598.

(10) Stanley, K.; Baird, M. C. *J. Am. Chem. Soc.* **1977**, *99*, 1808.

(11) Cameron, A. D.; Baird, M. C. *J. Chem. Soc., Dalton Trans.* **1985**, 2691.

(12) Hunter, B. K.; Baird, M. C. *Organometallics* **1985**, *4*, 1481.

(13) Ayscough, A. P.; Davies, S. G. *J. Chem. Soc., Chem. Commun.* **1986**, 1648.

(14) Reger, D. L.; Klaeren, S. A.; Lebioda, L. *Organometallics* **1986**, *5*, 1072.

(15) Georgiou, S.; Gladysz, J. A. *Tetrahedron* **1986**, *42*, 1109.

0002-7863/87/1509-5711$01.50/0 